

## Compositional characterization of iron gall inks in manuscripts using non-destructive techniques

Rita de Figueiredo Viegas

Under supervision of Prof. Maria Teresa Haderer de la Peña Stadler and Dr. Victoria Corregidor Berdasco

---

### Abstract

This work aims to characterize the elemental and molecular composition of iron gall inks and papers by means of several non-destructive techniques as: Particle Induced X-ray Emission (PIXE), Rutherford Backscattering spectrometry (RBS), X-ray diffraction technique (XRD), and Fourier Transformed Infrared spectroscopy (FTIR). Ultraviolet (UV) and infrared (IR) photography were used for ink differentiation and detection of paper stains.

The basic ingredients of iron gall inks, besides water, are: iron sulphate (vitriol), Arabic gum and tannins. By means of PIXE analysis, among other elements, sulphur, calcium and iron were identified. By XRD gallic acid and glucose were identified in the tannin sources and different iron sulphate hydrate compounds in the vitriol.

In papers written with the prepared inks, by RBS technique it was possible to identify light elements as oxygen and carbon. An estimation of ink depth profiling revealed ink penetration in the paper of the nanometer order. By XRD it was possible to identify calcite and cellulose.

After the determination of the right experimental conditions which assure the pristine conditions of the documents, different documents dated from the early XX century and belonging to a private collection were studied. Besides the elements listed above, traces of strontium and arsenic were identified in the documents' papers. Papers are mainly composed of cellulose and calcite. The FTIR analysis could however discriminate between ink and paper compounds.

**Keywords:** *Iron gall ink; PIXE; RBS; XRD; FTIR; UV and IR photography.*

---

### 1. Introduction

---

When studying ancient manuscripts it is of great interest to investigate about their origin and authenticity. Each writer usually had his personal ink recipes, each scribe usually had his own printing technique. The knowledge about paper manufacturing also may help in the identification of compounds when applying analytical techniques.

The manufacture of paper in Europe was first established in Islamic Spain in the middle of the 11<sup>th</sup> century, and in the second half of the 14<sup>th</sup> century the use of paper had become well accepted in Western Europe. In the beginning of the 19<sup>th</sup> century paper was made from cellulose and water by using hemp, flax and cotton fibers [1,2].

The inks have also evolved an evolution in their recipes and main ingredients. Carbon ink was the first documented ink and its first use is reported to circa 2500 BC [3]. The first appearance of iron gall ink is difficult to establish. Nevertheless, it can be safely stated that by the end of the late Middle Age iron gall ink was the primary ink chosen for writing in manuscripts [3].

A basic iron gall ink is created from four primary ingredients: tannin acid, vitriol (iron sulphate), gum Arabic and water. The tannin acid is extract from gall nuts containing Gallo tannins [4]. The iron sulphate (FeSO<sub>4</sub>), also known as vitriol or copperas, is obtained from minerals which contain many other metals as contaminants such as copper, aluminum, magnesium or zinc, which do not contribute to color of the ink solution. The third ingredient, gum Arabic, is a natural gum obtained from the Acacia tree. Gum Arabic is soluble in water (the fourth element), being its main purpose to bind the ink at the paper surface, producing a great brilliance and deep color [3].

Iron gall inks are known to influence the structure of cellulose fibers, causing deterioration of the paper or parchment. This motivates the quantitative investigation of the elemental and molecular composition of inks by the application of atomic and molecular techniques in order to predict and mitigate further degradation.

Techniques based on ion beam analysis (IBA) have been used for the study of ancient artifacts [5]. IBA techniques are nondestructive for most materials if external beam is used and they are complementary and usually can be implemented simultaneously. These techniques are multi-elemental, including light elements, they are quantitative and very sensitive and usually it is needed short time for each measurement. The nuclear microprobe allows the analysis of samples of any size and shape without any sample preparation and it avoids dehydration problems, reducing the risk of local heating and consequent damage [6,7]. Proton Induced X-ray Emission (PIXE) and Rutherford Backscattering Spectrometry (RBS) are two of the IBA techniques which can be used for characterization in the field of cultural heritage.

Particle Induced X-ray Emission (PIXE) technique was developed in 70ths. The pioneering works of PIXE using an external beam in documents belong to Davis' group, where the iron gall inks on the Gutenberg

Bible and on the Vinland map were studied [8,9]. External PIXE has revealed to be ideal for the analysis of inks in valuable documents as it provides a reliable quantitative measurement in a relatively short time and with little risk of damage.

PIXE cannot give any information about depth profiling of inks in paper which can help to understand more about ink corrosion processes in documents. For this purpose, Rutherford Backscattering Spectrometry (RBS) is an ideal technique to study elemental depth homogeneity and to study superficial layers containing heavy metals [10]. Furthermore, this technique also makes possible the identification of light elements that PIXE cannot detect (those with  $Z < 11$ ), such as oxygen and carbon, elements known to be part of paper compounds [1]. The possibility of employing PIXE and RBS simultaneously promotes the interest in using the last for the analysis of documents.

Near-infrared (NIR) reflectance and/or ultraviolet (UV) photography are used as complementary techniques to detect foxing and they also allow the perception of ink migrations and water stains in the manuscripts [11,12].

Despite IBA techniques, several other analytical techniques are used in the analysis of manuscripts, such as X-ray Diffraction (XRD) techniques and Fourier Transform Infrared (FTIR) spectroscopy. These techniques give the possibility of detecting the chemical compounds present in paper and inks.

XRD is a valuable technique for studying paper composition. Paper is composed of a matrix of cellulose and a variety of inorganic fillers added to confer the desired physical-mechanical properties. This technique allows to study both polymeric matrix and inorganic formulation of paper composition. The calculation of the crystallinity degree attained by the cellulose gives an idea of the quality level of paper, providing better conclusions about the conservation state of the document [13]

FTIR spectroscopy relies on the analysis of chemical bonds existent in the molecules that constitute the sample, allowing the identification of its compounds and so it is used for paper characterization [14,15].

---

## 2. Experimental setups

---

### 2.1. Proton Induced X-ray Emission

The PIXE measurements were performed with the external microprobe set-up of the CTN/IST facility, in Portugal. A Van de Graaff accelerator was used to produce the 2 MeV proton beam which is focused by means of set of quadrupole lenses reaching a final beam dimension of  $70 \times 70 \text{ mm}^2$ . The beam exit window consists on a  $\text{Si}_3\text{N}_4$  membrane with 100 nm thickness. An X-ray Si-SDD detector is placed at 2.8 cm from the sample at an angle of  $45^\circ$  to the beam direction. It has an active area of  $30 \text{ mm}^2$  and 145 eV resolution at 5.9 keV, during measurements a  $50 \text{ }\mu\text{m}$  foil of Mylar was placed in front of the detector. Documents were placed at 3 mm distance from the exit window with the guidance of two laser beams intersection. More details can be found on [16]. It is also possible to obtain elemental mapping as large as  $800 \times 800 \text{ }\mu\text{m}^2$  by scanning the sample with the micro-beam.

For this work the beam intensity was set at 300 pA and the acquisition time was 15 minutes for each measurement. Data acquisition and beam control is performed with the OMDAQ V5.2 software package. PIXE spectra evaluation and quantification was done with the GUPIX [17] software. During the analysis the samples were assumed as a thick homogeneous target.

### 2.2. Rutherford Backscattering Spectrometry

When the experiment was performed under vacuum conditions only the samples with no historical value were characterized. The samples were positioned at an incident angle of  $\alpha = 10^\circ$  with the beam direction and the data analyzed were collected thereby means of a particle detector placed at  $\theta = 165^\circ$ . The detector solid angle is 11,7 msr. Considering the elements to be analyzed (mostly Fe from the ink and Ca from the paper support which have a close atomic number), in order to increase the mass resolution of the technique, an alpha particle beam (2 MeV) was chosen to perform these measurements. The collected charges were  $1 \mu\text{C}$  and  $0.5 \mu\text{C}$  according to the sample. The SIMNRA software (version 6.06) was used to fit and analysis the obtained spectra and to calculate depth profiling [18].

### 2.3. X-ray Diffraction

In this work, the experiments were performed in two different diffractometers, the Hotbird [19] and the D8 Discover [20], both of them available at the CTN/IST. In both diffractometers the  $\theta$ - $2\theta$  geometry was used to determine interplanar distance of the planes parallel to the sample surface, acquire the x-ray diffraction spectra and then identify the compounds.

Both systems use Cu K $\alpha$ 1 monochromated radiation (1.540597 Å) as excited radiation beam, and a divergence slit (0.6mm) collimates the beam before traveling toward the sample. The samples are mounted on a 6-axes Eulerian cradle, making possible translation ( $x,y,z$ ) and rotation ( $\omega,\chi,\phi$ ) independent movements. The movement of the detector introduces another additional axis ( $2\theta$ ). The ( $\chi,\phi$ ) angles are normally used for the alignment of the samples, but they are not taking part in the XRD measurement. The  $\theta$  angle covers the whole 360° range while  $2\theta$  can be varied from -4° to 170°. The  $\theta/2\theta$  reproducibility is  $\pm 0.0001^\circ$ .

To reduce the divergence in the detector, the diffracted beam is passing through another (detector slit) of 0.32 mm. A scintillation NaI(Tl) detector receives the diffracted X-rays from the sample.

Usually, each diffractogram takes around 4 -5 hours to scan each sample and it were used two different softwares, Match! and PhasanX, to identify the compounds, together with the help of the Pearson's Database for crystalline compounds.

#### 2.4. Fourier Transformed Infrared Spectroscopy

The experiments were performed using a Thermo Scientific Nicolet IS50 FT-IR with ATR modulus available at the CTN/IST. The experiments were at room temperature and has a slide diamond crystal. The data was acquired in the 4000-400  $\text{cm}^{-1}$  range during 64 scans each round. The instrument has 4  $\text{cm}^{-1}$  of resolution. The time of acquisition of each spectrum is very low, approximately one minute.

For the study of the ingredients and the manufactured inks it were prepared samples in the form of pellets with potassium bromide (KBr). For the study of the documents, since they have large dimensions and don't fit in the chamber it was used the ATR (Attenuation Total Reflectance) method. The OMNIC software was used for spectra acquisition and data manipulation [21].

#### 2.5. IR and UV photography

A high resolution camera with a digital sensor (Nikon 5700) was used to record images under visible and UV illumination. The UV source is composed by 4 lamps of long wave UV light at 350 nm and they were oriented at 45° with the documents. NIR images were recorded with a Sony camera with a Carl Zeiss® Vario-Tessar lens.

### 3. Results and Discussions

#### 3.1. Ingredients

PIXE technique was the first to be performed in the ingredients. Except for the Arabic gum that only suffer the process of polish to create a flat area for analysis, pellets were used for the analysis of the rest of the ingredients. In the case of tannin it was used a commercial tannin already prepared in powder form.

As expected, the analysis revealed differences in the elemental composition of the ingredients. Figure 3.1 shows the PIXE spectra obtained for the three ingredients. In all X-ray energy spectra sulphur, chlorine, calcium and iron were identified. Additionally, potassium, titanium, copper, zinc and barium in the Arabic gum were identified. In iron sulphate pellet there were also identified manganese and zinc while the commercial tannin pellet has traces of potassium and titanium.

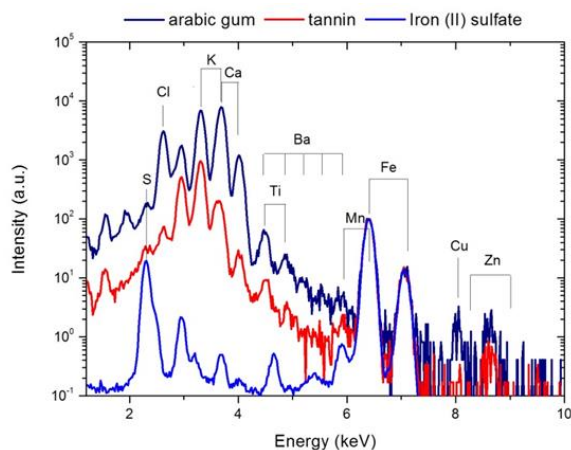


**Figure 3. 1.** X-ray energy spectra obtained from ingredients. The signals are normalized to the Fe-K $\alpha$  line.

Table 3.1 shows the ratios of the identified elements in the ingredients to get a better notion of the relative amount of each element.

**Table 3. 1.** Concentration ratios in iron gall inks main ingredients. ND: not detected.

|                   | S/Fe | Cl/Fe | K/Fe  | Ca/Fe | Ti/Fe | Mn/Fe | Cu/Fe | Zn/Fe | Ba/Fe |
|-------------------|------|-------|-------|-------|-------|-------|-------|-------|-------|
| Arabic gum        | 2,00 | 33,43 | 45,86 | 54,10 | 0,27  | ND    | 0,03  | 0,04  | 0,58  |
| Iron sulphate     | 1,00 | 0,01  | ND    | 0,01  | ND    | 0,01  | ND    | 0,01  | ND    |
| Commercial tannin | 0,47 | 0,53  | 6,45  | 1,14  | 0,05  | ND    | ND    | ND    | ND    |

From the analysis of table 3.1, we can conclude that Cl, K and Ca are the major constituents of the Arabic gum. In the case of iron sulphate, manganese and zinc may be considered contaminants since the ratios are low, in the order of  $10^{-3}$ . If we consider the result for the S/Fe ratio we can conclude that it has an excess of S, which is not in accordance with the chemical stoichiometry formula ( $\text{FeSO}_4$ ) and the atomic weight of these elements (32.07 and 55.85 for S and Fe, respectively).

XRD analysis were also performed in the ingredients. Figure 3.2 shows the diffractograms for the three sources of gallotannic acid, the iron sulphate pellet and the Arabic gum.

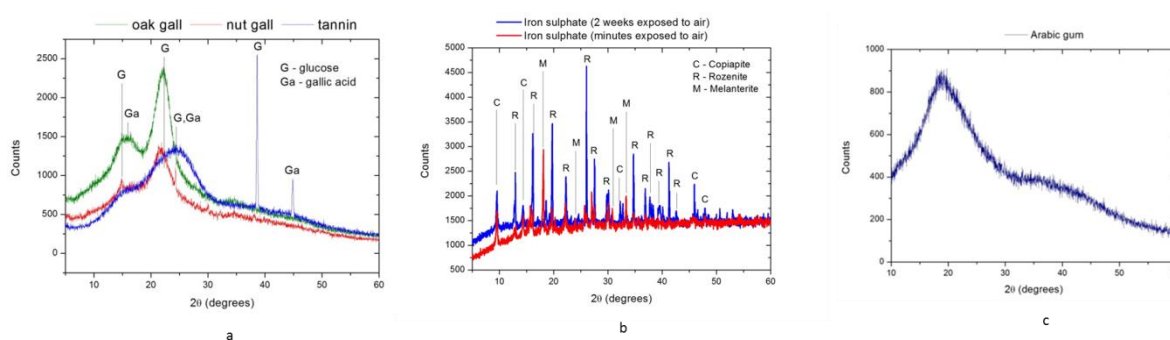


**Figure 3. 2.** X-ray diffraction patterns of tannins sources (a), iron sulphate pellets (b) and Arabic gum (c).

The natural sources of gallotannin acid (oak and nut galls) exhibit quite similar diffractograms while the commercial tannin shows a broader band centered a  $25^\circ$  and more intense peaks of glucose and gallic acid at higher angles.

In the case of the iron sulphate pellet produced two weeks before the measurements, which was in contact with the atmosphere, copiapite ( $\text{Fe}_{14}\text{O}_3(\text{SO}_4)_{18} \cdot 63\text{H}_2\text{O}$ ) and rozenite ( $\text{FeSO}_4 \cdot 4\text{H}_2\text{O}$ ) were identified. The other pellet also evidences copiapite but melanterite ( $\text{FeSO}_4 \cdot 7\text{H}_2\text{O}$ ) was identified instead of rozenite. The main difference in these molecules is the level of hydration they present. Therefore, the exposure to the atmosphere influences the chemical composition of this ingredient too, which can also influence the behavior of the iron gall inks.

The XRD results obtained for the Arabic gum (figure 3.2c) are similar to the ones found in the literature [22], where the diffraction pattern shows the amorphous nature of the gum with wide bands centered at  $18^\circ$  and  $35^\circ$ .

Regarding the FTIR analysis, measurements were performed for three ingredients: Arabic gum, iron sulphate and commercial tannin. Figure 3.3 shows the transmittance spectra obtained for the ingredients.

The identified peaks in the Arabic gum spectrum (figure 3.3a) are in accordance with the results found in the literature [23]. Concerning to the iron sulphate pellet (figure 3.3b), we see that peaks  $1101\text{ cm}^{-1}$  and  $536\text{ cm}^{-1}$  are indicative for the  $\text{SO}_4^{2-}$  ions, along with the peak at  $989\text{ cm}^{-1}$  [23]. Finally, some peaks were possible to identify in the commercial tannin FTIR spectrum. It was already verified the identification of gallic acid the XRD analysis of this ingredient (figure 3.2a) and the peaks observed in the transmittance spectrum in figure 3.3c are correspondent to this compound [23].

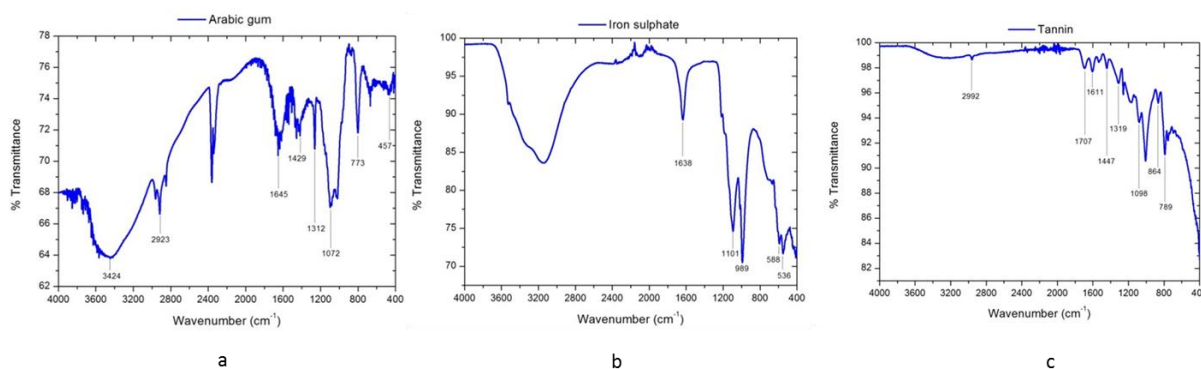


**Figure 3. 3.** FTIR spectra for Arabic gum (a), iron sulphate pellet (b) and tannin pellet (c).

### 3.2. Manufactured inks following recipes

Six different iron gall ink recipes were used to produce new inks. The inks were applied to modern paper just after their production, and then analyzed.

The PIXE analysis was performed in papers written with the six different recipes in order to study elemental composition of inks: inks from recipes 1,2 and 3 were written in paper1; inks from recipes 3nut and 3oak were written in paper3 and the ink from recipe 4 was written in paper 4. Analysis on paper were also done in order to discriminate the signals (figure 3.4a).

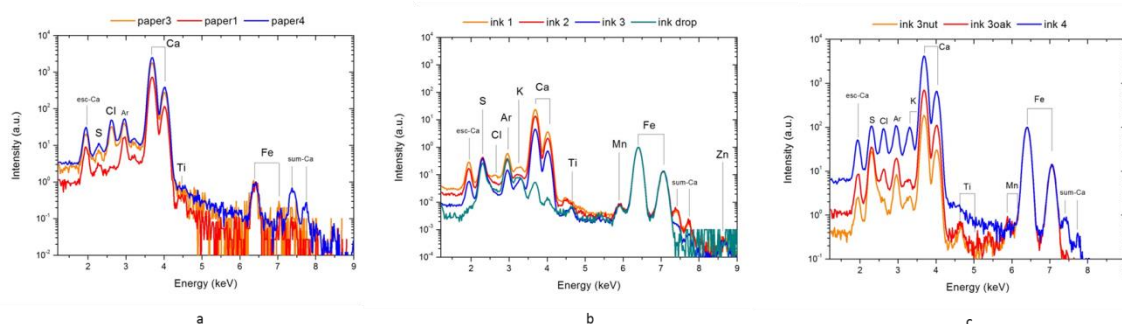


**Figure 3. 4.** X-ray energy spectra of three papers used as support of the six made iron gall inks (a), of the three iron gall inks recipes using commercial tannins (b) and of three iron gall inks recipes using natural tannins (c). The signal is normalized to the Fe-K $\alpha$  line.

Sulphur, chlorine, potassium, calcium and iron were identified in all inks in figure 3.4b. Only potassium and manganese were not identified in bare paper and so it is correct to assume that these elements belong to the inks. Despite the different tannin sources, it is clear from figures 3.4b and 3.4c that the elemental composition of the different inks does not vary except for the case of “ink3” which was the only one where zinc was identified, although in low concentration.

Concerning to the ink drop, it was manufactured with the three ingredients following the recipe of ink 1. The only difference is concerned to the fact that the ink drop has no contribution of elemental composition of the paper and so the signal of Ca is very low compared to the signal of “ink1”.

In order to characterize the manufactured iron gall inks and paper in terms of compound composition we choose to do XRD analysis. Figure 3.5 shows the X-ray diffraction patterns of the six samples of iron gall inks on the paper support. All spectra show the same peaks identified as compounds belonging to paper support. In the papers, two types of cellulose, I and II, were identified and it was also possible to identify calcite, the most stable polymorph of calcium carbonate (CaCO<sub>3</sub>), which is used as filler in paper manufacturing process [24].

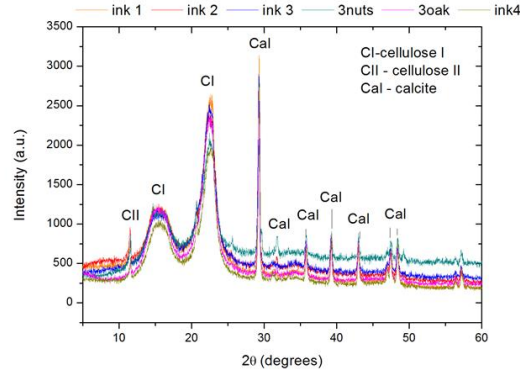


**Figure 3. 5.** X-ray diffraction patterns of six iron gall inks samples in paper.

The Crystallinity Index ( $CrI$ ) suggested by Segal and co-workers [25] is given by:

$$CrI = \frac{(I_{002} - I_{am})}{I_{002}} \times 100 \quad (4.1)$$

where  $I_{002}$  is the intensity of the crystalline peak at the maximum at  $2\theta$  between  $22^\circ$  and  $23^\circ$  for cellulose I and  $I_{am}$  is the intensity of the amorphous reflection at the minimum at  $2\theta$  between  $18^\circ$  and  $19^\circ$  for cellulose I. Values of  $CrI$  lower than those typical of cellulose (more than 80%) indicate a degraded material or a paper made of low-quality cellulose fibers, such as those coming from woods [26].

In table 3.2 are presented the correspondent Crystallinity Index for each of the six samples analyzed through XRD and also the values for the papers without inks.

**Table 3. 2.** Crystallinity Index ( $CrI$ ) for the papers written with the six ink recipes analyzed and the same papers unwritten.

| Sample | $CrI$ (%)        |              |
|--------|------------------|--------------|
|        | <i>ink+paper</i> | <i>paper</i> |
| 1      | 75,88            | 81,43        |
| 2      | 71,65            |              |
| 3      | 74,80            |              |
| 3oak   | 77,01            | 74,32        |
| 3nuts  | 67,81            |              |
| 4      | 75,09            | 82,34        |

Despite the approximated results between the Crystallinity Index for ink+paper and bare paper, we see that the percentages are lower in the case of paper written with iron gall inks. This fact is direct consequence of the ink interaction with the paper cellulose fibers, even after short time interaction. Moreover, from the results of  $CrI$  obtained for bare paper we may only assume that paper used has support for inks “3oak” and “3nuts” (paper 3) is made of low quality raw materials.

To have a better notion of the behavior of the ink in paper, it may be helpful to have an idea of its spread inside the paper. For this purpose, RBS was performed in the six samples (bare and inked papers). During simulations, it was assumed a layered target, being the substrate composed by cellulose ( $C_6H_{10}O_5$ ) and calcite (composition extracted from the simulation of the RBS spectrum recorded on the bare paper), and the first layer a mixture between iron ink (simulated as  $FeSO_4$ ) and cellulose+calcite. Also, elements as Cl, Na, Mg and N in low quantities were incorporated in the analysis to obtain a good fit, considering the elements added to manufacture paper [24] and the PIXE data.

Table 3.3 gives the values obtained for an estimation of the depth penetration of the six iron gall inks ( $FeSO_4$ ) in paper, considering the depth estimated for the 1<sup>st</sup> layer.

**Table 3. 3.** Estimation of the depth penetration of iron gall inks (considering only the  $\text{FeSO}_4$  ingredient) in paper. Only the depth of the 1<sup>st</sup> layer was used for the calculations.

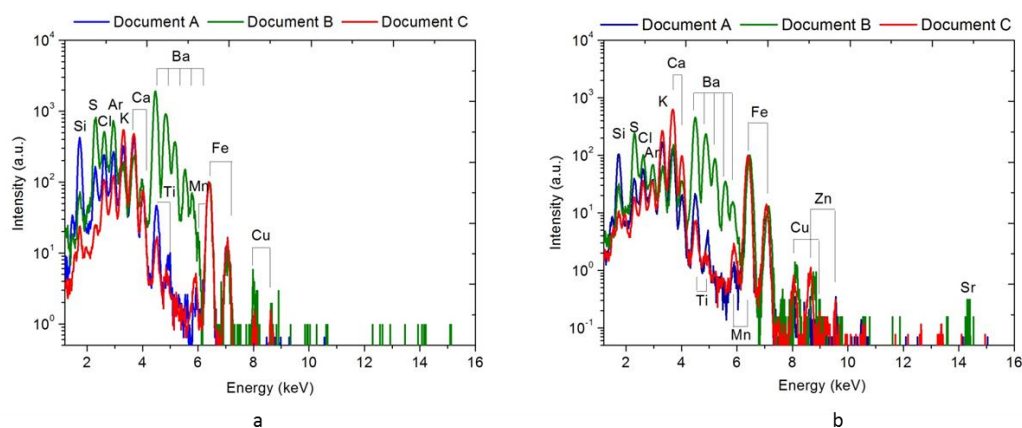
| inks | Depth 1 <sup>st</sup> layer ( $10^{15}$ atoms/cm <sup>2</sup> ) | Depth penetration of $\text{FeSO}_4$ (nm) |
|------|---|---|
| ink1 | 1500  | 41  |
| ink2 | 900   | 14  |
| ink3 | 10000   | 450                                       |
| 3nut | 500   | 32  |
| 3oak | 10000   | 570                                       |
| ink4 | 900   | 42  |

The calculations were made having into account the density of  $\text{FeSO}_4$  ( $1.898 \text{ g/cm}^3$ ) and the concentrations of iron, sulphur and oxygen in this layer. It was considered that the 1<sup>st</sup> layer was only ink and so the concentrations determined for the mentioned elements contribute to the iron sulphate molecule. As it can be seen, ink penetration is of the order of nanometers.

### 3.3. Analysis of documents from the beginning of the XX century

The documents studied in this work belong to a private collection. We chose five documents dated from the beginning of the 20<sup>th</sup> century and from Rio de Janeiro, Brazil. The documents are in good state of conservation and apparently don't show many signs of ink corrosion and paper degradation, although some documents present holes related to degradation.

Representative X-ray spectra of documents A, B and C are shown in figures 3.6a and 3.6b, obtained in uncovered paper and in ink covered regions, respectively.

**Figure 3. 6.** X-ray energy spectra obtained from non-inked (a) and inked areas (b) in documents A, B and C. The signal is normalized to the  $\text{Fe-K}\alpha$  line.

Concerning to the composition of papers analysed (figure 3.6a), some differences were detected among them. In all of them Ti was detected which can be attributed to titanium dioxide ( $\text{TiO}_2$ ), widely used as a white pigment or bleaching agent in paper [24]. In document B, the PIXE spectrum in figure 3.6a shows the presence of barium as one of the elements with higher concentration. Barium is an indicator of industrial paper manufacture [24].

PIXE analyses of inked areas in the documents (figure 3.6b) detected other elements besides S and Fe in concentrations that might be considered willful added to the inks. In Document B it were identified copper, zinc and strontium as elements present in inked areas (figure 3.6b). Document C (dated from 1897) has traces of manganese, zinc and copper in inked areas.

Clear differences in paper color and appearance between the documents A,B and C were emphasized by means of UV photography (figure 3.7). In general, the three documents fluoresces faintly whitish, being the document A (the one with the highest amount of Ti) the one with the highest glow signal. The paper from document B appears to be darkish than the other two documents under UV light, fact that probably result from the presence of barium in its composition.



**Figure 3. 7.** UV photography of Document A (right side), Document B (left side) and Document C (down in the picture).

The X-ray energy spectra for non-inked and inked areas in documents D and E are shown in figure 3.8.

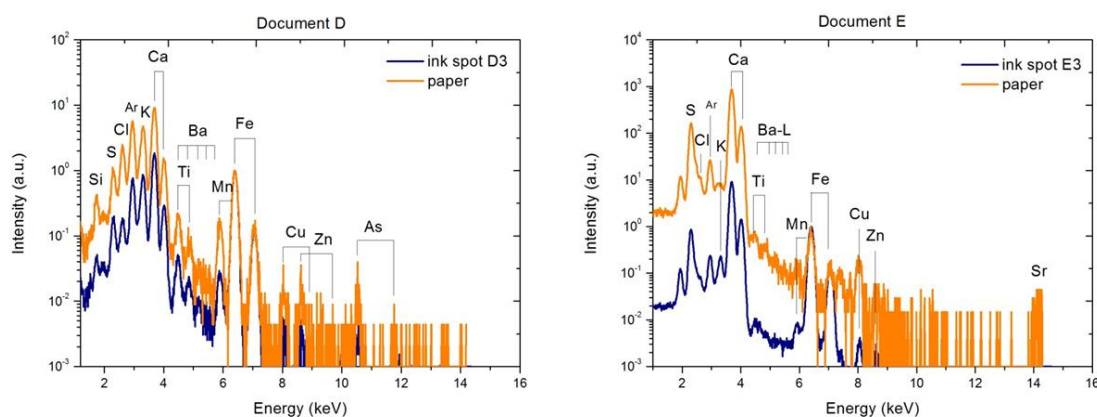


**Figure 3. 8.** X-ray spectra for non-inked and inked areas in document D and document E.

Paper elemental composition for document D is quite similar to document B considering the identified elements, apart from arsenic that was identified in this paper.

In document E, contrary to the other analyzed documents, silicon was not identified in neither in inked and non-inked areas. Silicon appears as a constituent of various compounds related to coating sizing in paper manufacturing [27]. The nonexistence of silicon in this document might be an indication that the paper suffered a total different manufacturing process.

Despite sulphur and iron, there were identified copper and zinc in the inked areas of both documents.

Table 3.4 is a summary of the identified compounds in the four documents analyzed through XRD.

**Table 3. 4.** Summary of the identified compounds in the four documents analyzed.

|            | Cellulose I | Cellulose II | Cellulose III | Kaolin | Calcite | Anhydrite | Baryte |
|------------|-------------|--------------|---------------|--------|---------|-----------|--------|
| Document A | •           | •            |               |        | •       |           |        |
| Document B | •           | •            |               |        | •       | •         | •      |
| Document D | •           |              | •             | •      | •       | •         | •      |
| Document E | •           |              | •             | •      | •       | •         |        |

In all documents, cellulose I was identified while cellulose II was identified only in documents A and B and cellulose III was found in documents D and E.

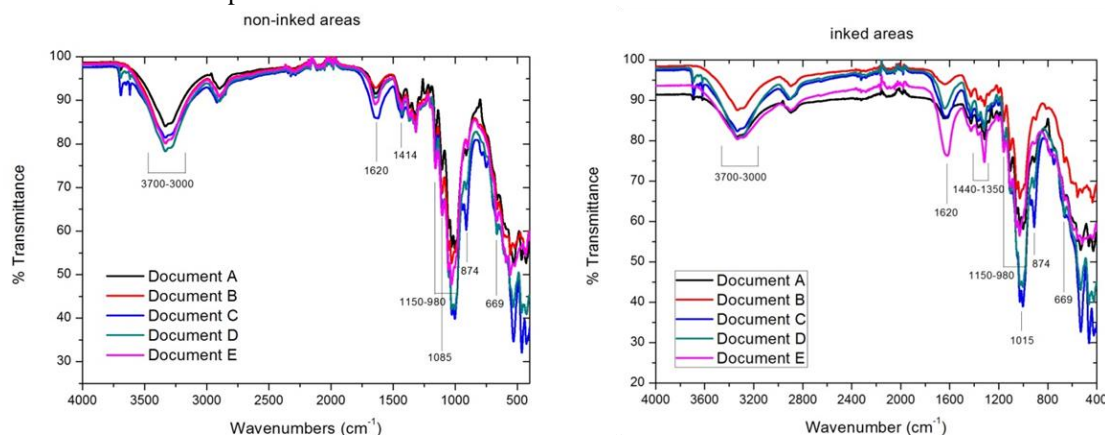
As in the case of iron gall ink recipes, the Crystallinity Index,  $CrI$ , for each document was also calculated in the inked areas and bare paper. In table 3.5 are the  $CrI$  values calculated considering the peaks from cellulose I. In all documents it can be concluded that the values for the Crystallinity Index for the samples of paper written with iron gall inks are lower than for bare paper.

**Table 3. 5.** Crystallinity Index (*CrI*) for the documents analyzed on inked and non-inked regions, considering the peaks from cellulose I.

| Paper sample | <i>CrI</i> (%)   |              |
|--------------|------------------|--------------|
|              | <i>ink+paper</i> | <i>paper</i> |
| Document A   | 77,72            | 80,33        |
| Document B   | 76,67            | 80,33        |
| Document D   | 84,71            | 89,45        |
| Document E   | 84,49            | 90,60        |

The Crystallinity Index are considerable high, above 80% for documents D and E even for ink+paper. When comparing the values for bare papers with the ones obtained in actual papers (table 3.2), we can assure that we are dealing with old but high quality papers which inherit the high quality of the raw materials used, if we consider the aging and corrosion processes of the documents, for instance the presence of foxing stains.

To study the chemical composition, FTIR analyses were performed in all the documents. Figure 3.9 shows the transmittance spectra for non-inked and inked areas.

**Figure 3. 9.** FTIR spectra for non-inked and inked areas of the documents.

In both figures, the C-OH and C-O-C groups from cellulose exhibit transmittance bands at  $3450\text{ cm}^{-1}$  and in the  $1150\text{-}980\text{ cm}^{-1}$  due to the O-H stretching of intermolecular hydrogen bonded hydroxyl groups and C-O-C stretch, respectively [28,29]. Calcite has correspondent peaks at around  $1414\text{ cm}^{-1}$  and  $1085\text{ cm}^{-1}$  and  $874\text{ cm}^{-1}$  [30,31].

Considering only the spectra for inked areas, the chemical bond  $\text{S}(=\text{O})_2$  exhibit transmittance band at the region between  $1440\text{-}1350\text{ cm}^{-1}$  [29].

#### 4. Conclusions

The study of elemental and molecular composition of iron gall inks by means of nondestructive techniques was well succeeded.

PIXE technique using an external proton beam was performed in manuscripts for the first time in Portugal, using the set-up installed at Campus Tecnológico e Nuclear, IST. The optimal experimental conditions are a beam current of 300 pA and an acquisition time of about 15-20 minutes, to assure the pristine conditions of the documents after the measurements.

XRD analysis of the ingredients allowed the identification of gallic acid and glucose in the three types of tannin sources used and different hydrate iron sulphur compounds (copiapite, rozenite and melanterite) in the vitriol. FTIR analysis allowed the identification of peaks associated to gallic acid in the tannin source and melanterite in the vitriol source.

XRD analysis of the produced inks provided the identification of celluloses I and II and calcite as constituents of paper. By RBS analysis, the penetration depth of the inks was calculated, values in the order of nanometers were found. The influence of the inks in the cellulose fibers of the papers was estimated considering their crystallinity index. In general, it was observed lower values for the inked areas which can be related to corrosion processes.

The characterization of the five documents from the beginning of the XX century, end of the XIX century, by means of their elemental and chemical composition was accomplished. By PIXE it was possible to

distinguish between different papers and manufacturing processes, because of the identification of key elements, such as barium, arsenic and strontium. By means of UV and IR photography, it was also possible to differentiate between papers as well as to recognize foxing and water stains in all the three documents.

The papers from the documents come from good quality materials since their crystallinity index is higher than 80%. By XRD analysis it was possible to identify three types of celluloses: cellulose I, II and III. Calcite, barite, anhydrite and kaolin were also identified. With FTIR it was not possible to identify other elements than those already identified through XRD in the papers but this technique helped to corroborate the previous results.

## References

- [1] R. M. Ion et al., Spectral Analysis of Original and Restored Ancient Paper from Romanian Gospel, *Rom. Journ. Phys.* 53, 2008, pp. 781-791.
- [2] M. Manso et al., Application of spectroscopic techniques for the study of paper documents: A survey, *Spectrochimica Acta Part B* 64, 2009, pp. 482-490.
- [3] [http://irongallink.org/igi\\_index8a92.html](http://irongallink.org/igi_index8a92.html) (March, 2014).
- [4] <http://www.alvissaras.50webs.com/eanes.html> (March, 2014).
- [5] L. Beck, L. Pichon, B. Moignard, T. Guillou, P. Walter, IBA techniques: Examples of useful combinations for the characterization of cultural heritage materials, *Nuclear Instruments and Methods in Physics Research B*, 269, 2011, pp. 2999-3005.
- [6] T. Calligaro, J.C. Dran, J. Salomon, P. Walter, Review of accelerator gadgets for art and archaeology, *Nuclear Instruments and Methods in Physics Research B*, 226, 2004, pp. 29-37.
- [7] S.A.E Johansson, J.L. Campbell, PIXE: A Novel Technique for Elemental Analysis, John Wiley & Sons, 1988.
- [8] T.A. Cahill, R.N. Schwab, B.H. Kusko, R.A. Eldred, G. Möller, D. Dutschke, D.L. Wick, A.S. Pooley, The Vinland Map, Revisited: New Compositional Evidence on Its Inks and Parchment, *Analytical Chemistry*, 59, 1987, pp. 829-833.
- [9] B.H. Kusko, T.A. Cahill, R.A. Eldred, R.N. Schwab, Proton Milliprobe Analysis of the Gutenberg Bible, *Nuclear Instruments and Methods in Physics Research B*, 3, 1984, pp. 689-694.
- [10] G. Demortier, A. Adriaens, Ion Beam Study of Art and Archaeological Objects, Office for Official Publications of the European Communities, Brussels, 2000, p. 9.
- [11] G. Verhoeven, Imaging the invisible using modified digital still cameras for straightforward and low-cost archaeological near-infrared photography, *Journal of Archaeological Science* 35, 2008, pp. 3087-3100.
- [12] I. Montani et al., Enhancement of writings on a damaged medieval manuscript using ultraviolet imaging, *Journal of Cultural Heritage* 13, 2012, pp. 226-228.
- [13] V. Causin et al., Forensic differentiation of paper by X-ray diffraction and infrared spectroscopy, *Forensic Science International* 197, 2010, pp. 70-74.
- [14] G. Bitossi et al., Spectroscopic techniques in cultural heritage conservation: A survey, *Appl. Spectrosc. Rev.* 40, 2005, pp.187-228.
- [15] A. Gorassini et al., Fourier Transformed Infrared Spectroscopy (FTIR) Analysis of Historic Paper Documents as a Preliminary Step for Chemometrical Analysis, CMA4CH 2008, Mediterranean Meeting.
- [16] V. Corregidor, L.C. Alves, P.A. Rodrigues, M. Vilarigues, R.C. Silva, The External Ion Beam Facility in Portugal for Studying Cultural Heritage, *e-Conservation Magazine*, 22, 2011, pp. 40-52.
- [17] J.A. Maxwell, W.J. Teesdale, J.L. Campbell, The Guelph PIXE software package II, *Nuclear Instruments and Methods in Physics Research, B*, 95, 1995, p. 407.
- [18] <http://home.rzg.mpg.de/~mam/> (March, 2014)
- [19] [http://www.itn.pt/facilities/uk\\_hotbird.htm](http://www.itn.pt/facilities/uk_hotbird.htm)
- [20] <https://fys.kuleuven.be/iks/nvsf/experimental-facilities/x-ray-diffraction-2013-bruker-d8-discover>
- [21] <http://www.thermoscientific.com/en/product/omnic-series-software.html>
- [22] K. C. S. Andrade; C. W. P. de Carvalho; C. Y. Takeiti; H. M. C. de Azeredo; J. da S. Corrêa; C. M. Caldas, Goma de cajueiro (Anacardium occidentale): Avaliação das modificações químicas e físicas por extrusão termoplástica, *Polímeros vol.23 no.5 São Carlos*, 2013.
- [23] M. Ursescu, T. Măluțan, S. Ciovică, Iron gall inks influence on papers' thermal degradation, *European Journal of Science and Theology*, 2009, Vol.5, No.3, pp. 71-84.
- [24]<http://www.paperonweb.com/chemical.html>
- [25] L. Segal et al., An empirical method for estimating the degree of crystallinity of native cellulose using the X-ray diffractometer, *Textile Research Journal* 29, 1959, pp. 786-794.
- [26] Nicoleta Terinte, Roger Ibbett, Kurt Christian Schuster, Overview on native cellulose and microcrystalline cellulose I structure studied by X-ray diffraction,(WAXD): comparison between measurement techniques, *Lenzinger Berichte* 89, 2011, pp. 118-131.
- [27] <http://www.paperonweb.com/chemical.html> (March, 2014)
- [28] N. Rangelova, L. Radev, S. Nenkova, I. M. Miranda Salvado, M. H. Vas Fernandes, M. Herzog, Methylcellulose/SiO<sub>2</sub> hybrids: sol-gel preparation and characterization by XRD, FTIR and AFM, *Cent. Eur. J. Chem.* 9(1) (2011), pp. 112-118.
- [29] Sadtler, The Infrared Spectra Atlas of monomers and polymers, Sadtler Research Laboratories, 1980.
- [30] A. Gorassini, P. Calvini, A. Baldin, Fourier Transformed Infrared Spectroscopy (FTIR) Analysis of Historic Paper Documents as a Preliminary Step for Chemometrical Analysis, CMA4CH 2008, Mediterranean Meeting
- [31] R. M. Ion, M. L. Ion, V. I. R. Niculescu, I. Dumitriu, R. C. Fierascu, G. Florea, C. Bercu, S. Serban, Spectral Analysis of Original and Restored Ancient Paper from Romanian Gospel, *Rom. Journ. Phys.* 53, 2008, pp. 781-791.